



## Phase Transition in Conjugate Planes of Charged AdS Black Hole

Nguyen Tuan Anh<sup>1</sup>, Tran Huu Phat<sup>2</sup>, Hoang Van Quyet<sup>3\*</sup>

<sup>1</sup>Faculty of Energy Technology, Electric Power University, 235 Hoang Quoc Viet, Hanoi, Vietnam

<sup>2</sup>Vietnam Atomic Energy Commission, 59 Ly Thuong Kiet, Hanoi, Vietnam

<sup>3</sup>Department of Physics, Hanoi Pedagogical University 2,

32 Nguyen Van Linh St, Xuan Hoa ward, Phuc Yen city, Vinh Phuc province

**Abstract:** In this study, possible patterns of phase transitions at finite temperature in the charged AdS black holes (BHs) are investigated. It is shown that in corresponding to standard pairs of conjugate thermodynamic variables charged AdS black holes contains either critical phenomena or interesting phase behaviour: a) for volume vs. pressure ( $V, P$ ), a first order phase transition occurs similar to the van der Waals like from liquid to gas; b) for electric potential vs. charge ( $\Phi, Q$ ), a first order phase transition associated with the electric charge instability. The distinction between them is characterized by the behaviors of the phase diagrams, the phase transition regions, the latent heats, the coexistence lines and the scalar curvatures associating with different Riemann spaces established in BH thermodynamic geometry approach. This scenario could become realistic for all other black holes.

**Keywords:** AdS black holes, phase transitions, van der Waals -like, thermodynamic geometry.

### I. INTRODUCTION

It is known that the metric of the four dimensional RN–AdS BH has the form

$$ds^2 = -f(r)dt^2 + \frac{dr^2}{f(r)} + r^2 d\Omega_{2,k}^2. \quad (1)$$

Where:

$$d\Omega_2^2 = d\theta^2 + \sin^2 \theta d\phi^2, \quad (2)$$

$$f = 1 - \frac{2kM}{r} + \frac{Q^2}{r^2} + \frac{r^2}{\ell^2}. \quad (3)$$

In (1)  $d\Omega_2^2$  is the metric of a two – sphere  $S^2$  of radius 1. The parameters  $M$  and  $Q$  are related to the mass and charge of BH by corresponding factors. The horizon is defined as the largest root of the equation.

$$f(r_+) = 1 - \frac{2M}{r_+} + \frac{Q^2}{r_+^2} + \frac{r_+^2}{\ell^2} = 0. \quad (4)$$

From Eq (4) we have:

$$M = \frac{r_+}{2} + \frac{Q^2}{2r_+} + \frac{r_+^3}{2\ell^2}. \quad (5)$$

The phase transition from small – large BHs given by (1) and (5) was proven to be similar to the phase transition from liquid to gases in the van der Waals theory [1] after the cosmological constant was identified to the thermodynamic pressure  $P$ .

$$P = -\frac{\Lambda}{8\pi} = \frac{3}{8\pi\ell^2}. \quad (6)$$

The temperature and entropy of BH can be easily derived by taking into account (5) and (6)

$$T = \frac{f'(r)}{4\pi} \Big|_{r=r_+} = \frac{1}{4\pi r_+} \left( 1 - \frac{Q^2}{r_+^2} + \frac{3r_+^2}{\ell^2} \right). \quad (7)$$

$$S = \pi r_+^2. \quad (8)$$

In this set up,  $M$  turns out to be the enthalpy of BH. The extended first law of the BH thermodynamics [4, 5] is expressed by introducing the topological charge  $\varepsilon = 4\pi$  as in Refs. [2, 3].

$$dM = TdS + \Phi dQ + VdP. \quad (9)$$

Eq. (9) shows that the volume  $V = 4\pi r_+^3 / 3$  is conjugated to pressure  $P$  and the electric potential  $\Phi = Q / r_+$  is conjugated to charge  $Q$ .

This paper is organized as follows. In Section 2 the phase transition patterns are investigated corresponding to standard pairs of conjugate thermodynamic variables of (9). The Section 3 is devoted to the Ruppeiner thermodynamic geometry which permits us understanding better the properties of phase transitions in BH. The conclusion is presented in the last Section 4.

## II. PHASE TRANSITION PATTERNS

### A. Phase transition in V- P plane

Based on (7) and (9) the BH equation of state gives

$$P = \left( \frac{\pi}{6} \right)^{1/3} \left[ \frac{T}{V^{1/3}} - \left( \frac{\pi}{6} \right)^{1/3} \frac{1}{2\pi V^{2/3}} + \frac{Q^2}{3V^{4/3}} \right], \quad (10)$$

at fixed  $Q$ .

The critical point of phase transition from small to large BHs is easily obtained.

$$P_c = \frac{1}{96\pi Q^2}, \quad V_c = \pm 8\sqrt{6}\pi Q^3, \quad T_c = \pm \frac{1}{3\sqrt{6}\pi Q}.$$

In order for the critical values have physical meaning (i.e. they are real),  $Q \neq 0$ , and sign  $+$  ( $-$ ) for  $Q > 0$  ( $Q < 0$ ).

At fixed  $Q$ , the ratio

$$\frac{P_c V_c}{T_c} = \frac{3\pi Q^2}{2}, \quad (11)$$

is a constant.

Using (9), (11) leads to

$$p = \frac{8\tau}{3v^{1/3}} + \frac{1}{v^{2/3}} \left( \frac{1}{3v^{1/3}} - 2 \right), \quad (12)$$

where  $p, v$ , and  $\tau$  are dimensionless variables,

$$p = P / P_c, \quad v = V / V_c, \quad \tau = T / T_c.$$

In the geometric units  $k_B = G_N = \hbar = c = 1$ . Here  $k_B, G_N$  are the Boltzmann and Newton gravitational constants, respectively. Then the P-V diagram of charged AdS BH is easily depicted in Fig. 1a at any arbitrary values of topological and electric charges Eq (11) is used here. This is the typical phase diagram of the van der Waals like in which the coexistence line for this phase transition is shown in Fig. 1b. The coexistence curve terminates at the critical point  $(P_c, T_c)$ . On crossing the curve from left to right the system changes similarly from pure liquid to pure gas. At a fixed pressure, small BH is in the region of lower temperature while large BH is at higher temperature. Similarly, at a fixed temperature, small BH is in higher pressure while large BH is in the lower pressure. This phase transition from small BH to large BH is the first order. This is clearly seen in Fig. 2a, the entropy  $S(T)$  is discontinuous at a definite value  $q(10)$  corresponding to the curve  $P < P_c$ . In

accordance with this, the latent heat was obtained.

$$\Delta H(T) = T[S_2(T) - S_1(T)],$$

The  $T$  dependence of which is represented in Fig. 2b. It coincides with Fig. 20 of Ref. [6]. The higher the gap, the lower the temperature vs critical value.

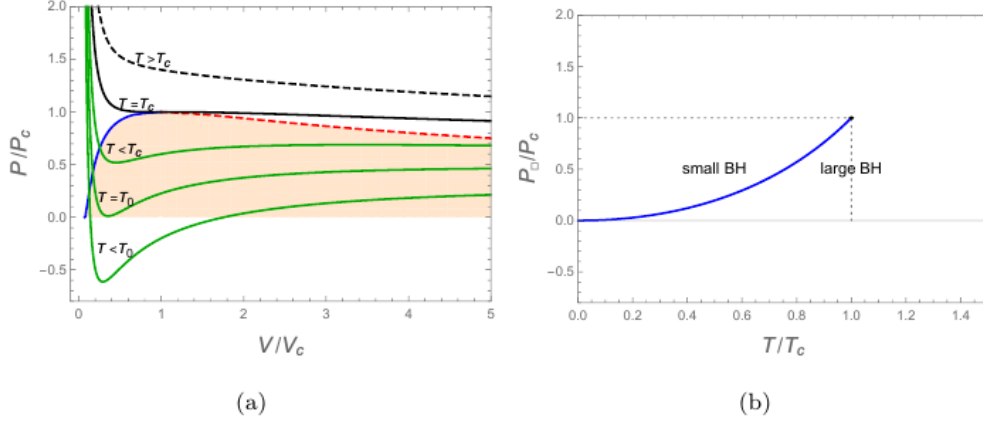


**Fig. 1.** (a) The equation of state in  $P$ - $V$  plane at any fixed  $Q$ , and (b) The coexistence line for small/large BHs transition. (Figures are plotted by the dimensionless variables, so the results are independent on choosing the values of  $Q$ )

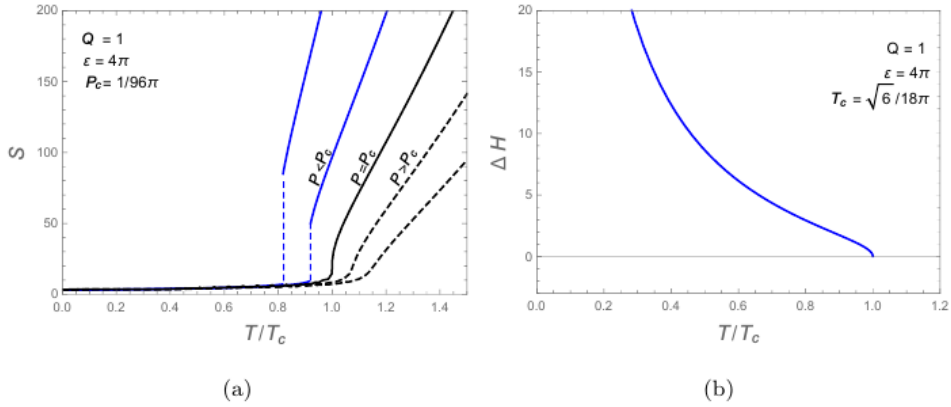


**Fig. 2.** The  $T$  dependence of the entropy  $S(T)$  (a) and latent heat  $\Delta H(T)$  at  $Q = 1$

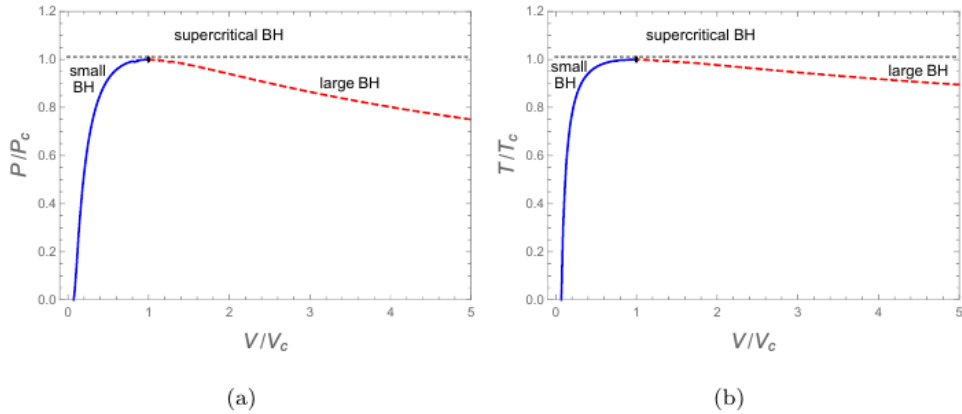


**Fig. 3.** The phase diagram in the  $P$ - $V$  plane (a) and in the  $T$ - $V$  plane (b)

Another facet of the SBH/LBH phase transition is shown in the Figs. 3a and 3b. This is the phase pattern in the  $P - V$  and  $T - V$  plane. These figures show that the phase transition occurs under the critical values of  $P$  and  $T$ .

The results Figs. (1, 2, 3) show that the small/large BHs transition happens below the critical point  $(P_c, T_c)$  in the case of fixed  $Q$ .

Those phase diagrams which associate with the electric charge instability and topological charge instability are scrutinized in detail.

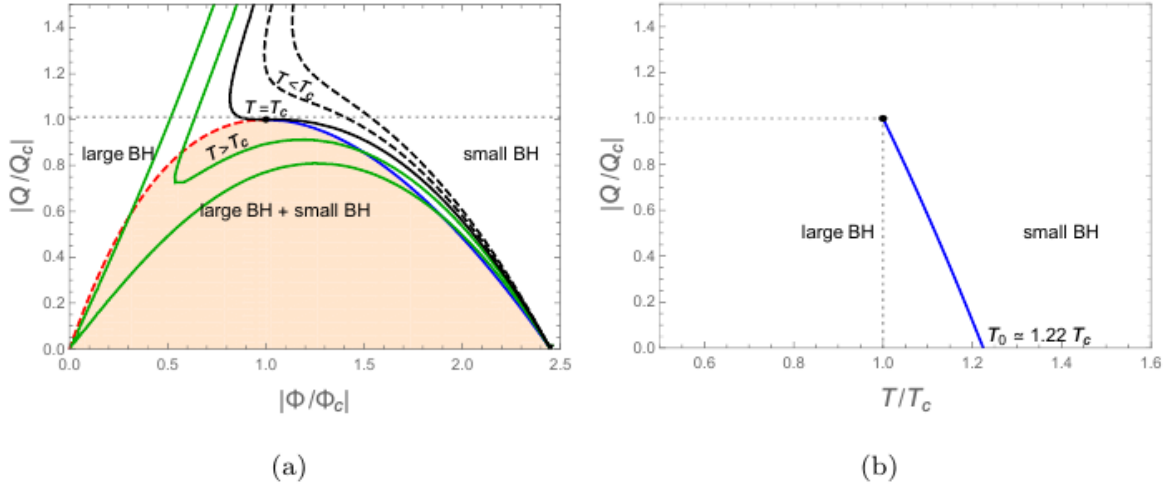


**Fig. 4.** (a) The equation of state in the  $Q-\Phi$  plane at several values of  $T$  and any fixed values of  $\epsilon, P$ , and (b) The coexistence line of the phase transition occurring in Fig. 4a. (Figures are plotted by the dimensionless variables, so the results are independent on choosing the values of  $P$

The critical point of EoS (13) is determined by:

$$Q_c = \frac{1}{4\sqrt{\pi}\sqrt{6P}}, \quad \Phi_c = \frac{1}{\sqrt{6\pi}}, \quad T_c = \frac{4\sqrt{P}}{3\sqrt{\pi}}, \quad (14)$$

Where  $P$  has fixed positive value in order that these critical values are real and positive. Equations (13) and (14) are then utilized, leading to

$$\left(q - \frac{4\tau\phi}{3}\right)^2 = \frac{\phi^2}{9} [16\tau^2 + 3(\phi^2 - 6)], \quad (15)$$

## B. Phase transition in $Q-\Phi$ plane

Based on (5) and (7) we obtain

$$\left(Q - \frac{T\Phi}{4P}\right)^2 = \frac{\Phi^2}{P} \left(\frac{T^2}{16P} - \frac{1}{8\pi} + \frac{\Phi^2}{8\pi}\right), \quad (13)$$

at fixed  $P$ .

The unstable region of the isothermal permittivity is constrained by:

$$\eta_T = \left(\frac{\partial Q}{\partial \Phi}\right)_T \gg 0,$$

which provides the evolution of  $Q$  versus  $\Phi$  at different values of  $T$  and fixed  $P$ .

Where  $q, \phi,$  and  $\tau$  are dimensionless variables,

$$q = Q/Q_c, \quad \phi = \Phi/\Phi_c, \quad \tau = T/T_c.$$

Eq. (14) gives

$$\frac{Q_c \Phi_c}{T_c} = \frac{1}{32P}. \quad (16)$$

Fig. 4a shows the phase diagram in the  $Q-\Phi$  plane at any fixed  $P$  (here Eq.(15) is used). It is notable that  $Q-\Phi$  are real and non-zero variables, i.e. may be positive or

negative.  $\Phi \sim Q$ , so  $\Phi > 0$  as  $Q > 0$ , and vice versa.

It is evident that Eq. (16) is quite different from (10). This difference tells that the phase transition, displayed in Fig. 4a, is the other type of the Van der Waals - like, in which the coexistence line of two phases is represented in Fig. 4b where two phases are in equilibrium.

Fig. 4b shows that, at a fixed electrical charge, large BH is in the region of lower temperature while small BH is at higher temperature. Similarly, at a fixed temperature, small BH has higher electrical charge while large BH has the lower charge. This phase

transition is also the first order since its corresponding latent heat is different to zero. Indeed, the  $T$  dependence of the entropy  $S$  as shown in Fig. 5a at  $P = 1/(8\pi)$ . The entropy  $S(T)$  is discontinuous at a definite value of  $T$  corresponding to the curve  $\pm Q < Q_c$ . Then we get the latent heat  $\Delta H(T)$  and its  $T$  dependence is shown Eq. (12), the behavior of this quantity totally reflects what displays in Fig. 5b. It is evident that this behavior of latent heat is in contrast with what is shown in Fig. 2b. Also, it is witnessed that a large distinction between Figs. 5a and 2a. In this case, the higher the gap, the higher the temperature vs critical value.

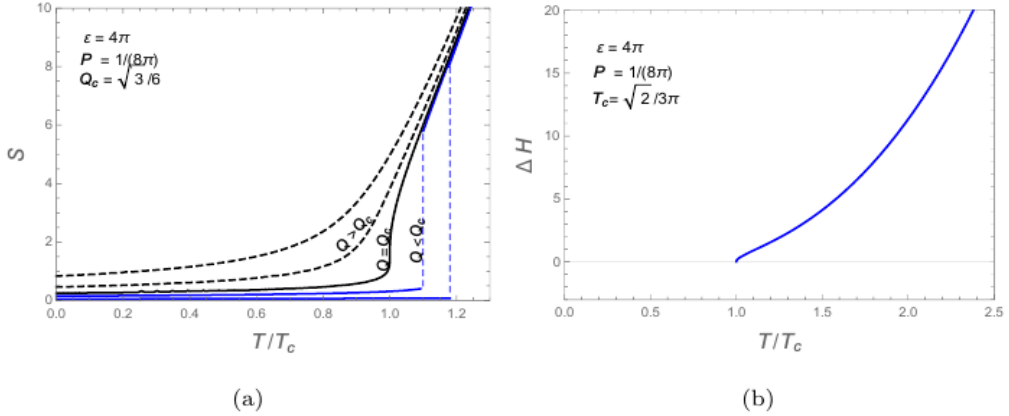


Fig. 5. The  $T$  dependence of the entropy (a) and the latent heat (b) at  $P = 1/(8\pi)$

Figure 6 provides support for the examination of phase patterns in the  $Q - \Phi$  and  $T - \Phi$  planes that exhibit the first-order phase

transition SBH/LBH. These figures show that the phase transition occurs below the critical value of  $Q$  but above the critical value of  $T$ .

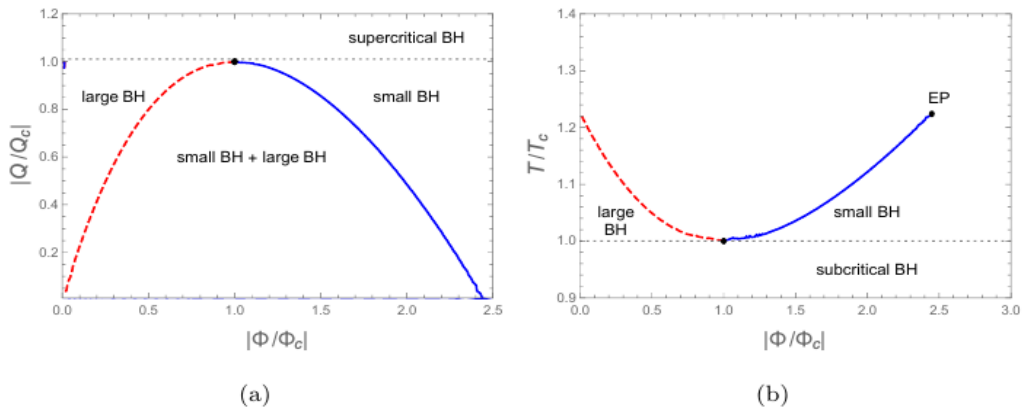


Fig. 6. The phase diagram in the  $Q - \Phi$  plane (a), and in the  $T - \Phi$  plane (b)

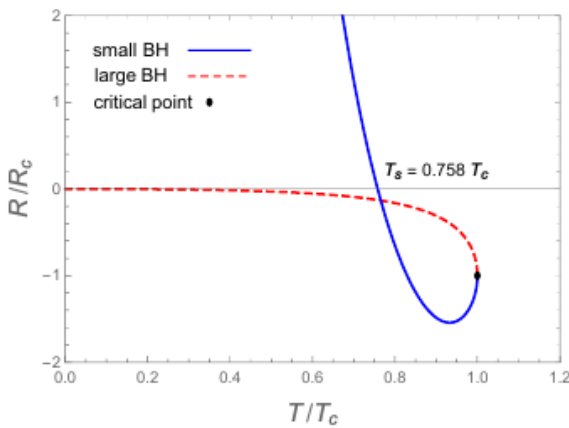
The results show that the small/large BHs transition happens below the critical point  $Q_c$  but above  $T_c$ , concretely, in the region  $Q \in (-Q_c, Q_c)$ ,  $T \in (T_c, 1.22 T_c)$ , and  $\Phi \in (-2.5 \Phi_c, 2.5 \Phi_c)$  at fixed  $P$ .

### III. THERMODYNAMIC GEOMETRY

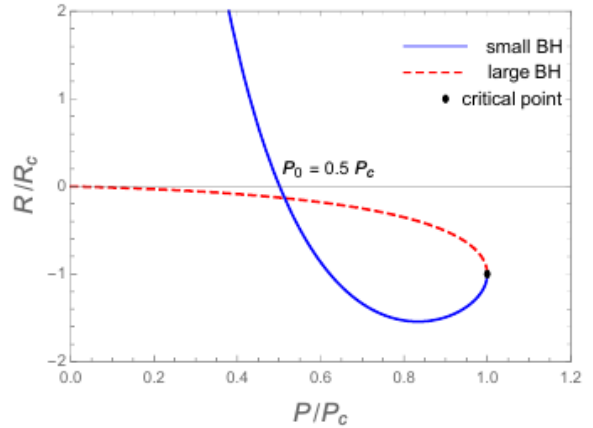
Making use of the thermodynamic geometry [7-9] the behavior of charged AdS black holes and the interaction forces between their micro-molecules were investigated in a lot of papers [10-15]. In this Section the interaction forces behave in different phase transitions studied in previous Section is observed. It is well known that the thermodynamic scalar  $R$  associated with BH provides us with important information related to the interaction forces between the BH micro-molecules [16-19]:

- Positive  $R$ ,  $R > 0$ , corresponds to a repulsive interaction.
- Negative  $R$ ,  $R < 0$ , corresponds to attractive interaction.
- Vanishing  $R$ ,  $R = 0$ , means that there is no interaction.

In this end, the Riemann space is given by:



(a)



(b)

**Fig. 7.** The dependence of  $R/R_c$  on  $T$  (a) and  $P$  (b)

$$ds^2 = \frac{\partial M}{\partial x^i \partial x^k} dx^i dx^k, i, k = 0, 1, \quad (17)$$

where  $M$  is the enthalpy of BH. Our investigation focuses on three cases:

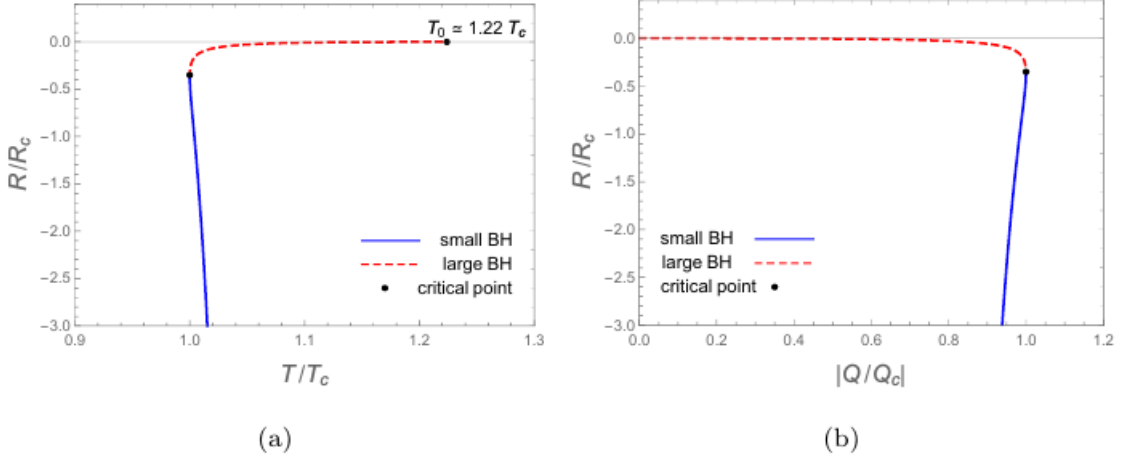
#### A. For the case $(V, P)$

As  $x^0 = V$  and  $x^1 = P$  for the transition corresponding to Fig.1, we obtain:

$$\frac{R}{R_c} = \frac{1 - 3v^{2/3}}{2\tau v^{5/3}}, \quad v = V/V_c, \quad \tau = T/T_c, \quad R_c = \frac{1}{12\pi Q^2}.$$

in which  $R_c$  is the value of  $R$  at critical values of corresponding arguments. The  $\tau$  dependence of  $R/R_c$  is plotted in Fig. 7. It indicates that for small BHs as  $T < 0.758 T_c$  and  $P < 0.5 P_c$  the interaction force is repulsive, then vanishes at  $T = 0.758 T_c$  and  $P = 0.5 P_c$ . As  $T$  belongs to the intervals  $(0.758 T_c, T_c)$  and  $(0.5 P_c, P_c)$  it turns out to be attractive. While this force is always attractive for large BHs.

Fig. 7 shows that the SBH/LBH phase transition only happens below  $T_c$  and  $P_c$  at fixed  $Q$ .

**B. For the case (  $\Phi, Q$  )**

**Fig. 8.** The dependence of  $R/R_c$  on  $T$  (a) and  $Q$  (b)

As  $x^0 = \Phi, x^1 = Q$  for the phase transition corresponding to Fig. 4a, we get:

$$\frac{R}{R_c} = \frac{\phi^5(8q\tau - 6\phi + \phi^3)(-128q^3\tau^3 + 16q^2\tau^2\phi(9 - 2\phi^2) + 12q\tau\phi^4B)}{2q^3\tau(-16q^2\tau^2 + 8q\tau\phi^3 - 6\phi^4 + \phi^6)^2},$$

where:

$$\phi = \Phi/\Phi_c, \quad q = Q/Q_c, \quad \tau = T/T_c, \quad B = (\phi^2 - 4) + \phi^5(\phi^2 - 6)(\phi^2 - 3), \quad R_c = 4P.$$

The  $\tau$  dependence of  $R/R_c$  is plotted in Fig. 11 which shows that the interaction force is totally attractive for all values of  $T$  and  $Q$ , and SBH/LBH phase transition occurs as  $T_c < T < 1.22 T_c$  and  $Q < Q_c$  at fixed  $P$ .

#### IV. CONCLUSION

By exploring the roles played by the thermodynamic quantities  $\Lambda$  and  $Q$  in the phase transitions of charged AdS black hole, all possible phase transitions of the charged BH are investigated systematically and the results are shown that there exist two different patterns of BH phase transitions which are featured by the behaviors of latent heats  $\Delta H(T)$ , the coexistence lines, the phase diagrams, the

interaction forces between micro-molecules and the ratios.

$$\frac{P_c V_c}{T_c} = \frac{3\pi}{2} \quad (18)$$

for the phase transition in the  $V$ - $P$  plane as choosing  $Q = 1$ ,

$$\frac{Q_c \Phi_c}{T_c} = \frac{\pi}{4} \quad (19)$$

for the phase transition in the  $Q$  -  $\Phi$  plane as choosing  $\Lambda = -1$ .

Eqs. (18) and (19) confirm that the constants (similar to ideal gas constant) are different for patterns. This means that they belong to different classes of the phase transition.

#### REFERENCES

- [1]. David Kubiznak, Robert B. Mann, Mae Teo, *Class. Quantum Grav.* **34**, 063001, 2017 and references herein.
- [2]. Y. Tian, X. N. Wu and H.B.Zhang, *JHEP* **10**, 170, 2014.
- [3]. Y.Tian, *Class. Quantum Grav.* **36**, 245001, 2019.

- [4]. Shan-Quan Lan, *Advances in High Energy Physics*, 4350287, 2018.
- [5]. J. M. Bardeen, B. Carter, S. W. Hawking, *Commun. Math. Phys.* **31**, 161, 1973.
- [6]. David C. Johnston, *Advances in Thermodynamics of the van der Waals Fluid*, Morgan & Claypool, San Rafael, CA, 2014.
- [7]. G.Ruppeiner *Rev. Mod. Phys.* **67**, 605 ( 1995) [Erratum-ibid. **68**, 313, 1996].
- [8]. G. Ruppeiner, *Phys. Rev. D* **78**, 024016 (2008).
- [9]. F. Weihold, *J. Chem. Phys.* **63**, 2479 (1975) [ Erratum-ibid.**63**,2484, 1975 ].
- [10].S.-W. Wei and Y.-X. Liu, *Phys. Rev. Lett.* **115**, 111302, 2015.
- [11].Y.-G. Miao and Z.-M. Xu, *Phys.Rev. D* **98**, 044001, 2018.
- [12].A.Dehyadegari, A.Sheykhi, and A.Montakhab, *Phys.Lett B* **768**, 235, 2017.
- [13].A.Dehyadegari, A.Sheykhi, and S.W.Wei, *Phys. Rev. D* **102**, 104013, 2020.
- [14].H.- Liu, H.-Lu , M.-X. Luo and K.-N. Shao, *JHEP* **12**, 054, 2010.
- [15].Sh.-W.Wei, Y.-X. Liu and R.B.Mann, *Phys.Rev.Lett.* **123**, 071103, 2019.
- [16].G.Ruppeiner, *Phys.Rev. E* **86**, 021130, 2012.
- [17].G.Ruppeiner, *Phys.Rev. E* **88**, 032123, 2013.
- [18]. G.Ruppeiner, *J.Phys.: Conf. Series* **410**,012138, 2013.
- [19]. G.Ruppeiner, *Springer Proc. Phys.* **153**, 179, 2014.
- [20]. Nguyen Tuan Anh, Tran Huu Phat, and Hoang Van Quyet, *The intermolecular forces in charged AdS black hole*, submitted to *Phys. Lett. B*, 2022.